



# Radiolabeling, docking studies, in silico ADME and biological evaluation of serotonin with $^{125}\text{I}$ for 5-HTRs imaging

Dina M. El-Sharawy<sup>1,3,5</sup> · Marwa S. El Refaye<sup>2,3</sup> · H. Hussien<sup>1,3</sup> · Asmaa M. AboulMagd<sup>4</sup>

Received: 13 April 2020 / Revised: 3 June 2020 / Accepted: 8 June 2020 / Published online: 4 August 2020

© China Science Publishing & Media Ltd. (Science Press), Shanghai Institute of Applied Physics, the Chinese Academy of Sciences, Chinese Nuclear Society and Springer Nature Singapore Pte Ltd. 2020

**Abstract** Serotonin is one of the significant signaling molecules used by several neural systems in the gut and brain. This study aimed to develop a novel and potent tracer for targeting, detecting, and imaging serotonin receptors (5-HTRs), which is a promising tool in the determination of the receptor's function and relationship with the diseases related to serotonin and its receptor dysfunction. Serotonin was effectively labeled via a direct electrophilic substitutional reaction using an oxidizing agent such as iodogen with  $^{125}\text{I}$  in a neutral medium, and  $^{125}\text{I}$ -serotonin was achieved with a maximum labeling yield of  $91 \pm 0.63\%$  with in vitro stability up to 24 h. Molecular modeling was conducted to signify  $^{125}\text{I}$ -serotonin structure and confirm that the radiolabeling process did not affect serotonin binding ability to its receptors. Biodistribution studies show that the maximum gastro intestinal tract uptake of  $^{125}\text{I}$ -serotonin was  $17.8 \pm 0.93\%$  ID/organ after

30 min postinjection and the tracer's ability to pass the blood–brain barrier. Thus,  $^{125}\text{I}$ -serotonin is a promising single photon emission computed tomography tracer in the detection of 5HTRs.

**Keywords** Serotonin · Electrophilic substitution · Molecular modeling · 5HTRs

## 1 Introduction

Serotonin is a monoamine central neurotransmitter that is involved in various physiological functions and psychiatric and neurologic disorders. Serotonin is a significant gastrointestinal molecule [1, 2]. It is a messenger induced by enterochromaffin cells in the intestinal mucosa [3, 4] and acts as a sensory transducer. It activates external and substantial afferent neurons for secretory and peristaltic responses, sensation of pain, nausea, and vomiting and information transfer to the central nervous system (CNS) [5–8]. It has a critical role as a neurotransmitter in the initiation and dissemination of impulses and brain-to-gut signaling [9]. The total serotonin level in the human body is approximately 10  $\mu\text{g}$ , in which about 5% are present in platelets and the CNS [10], The remaining serotonin level (95%) exists in the GIT [11–13]. The secreted serotonin is transported to the tissue through the platelet, which stores it. When the platelet conjugates to a clot, it releases the serotonin, leading to hemostasis regulation and blood clotting. Moreover, studies showed that there is a relationship between serotonin level and bone density. Pharmacologic studies classified serotonergic receptor families and subtypes into seven different classes (5-HT<sub>1–7</sub>) related to structural, functional, and pharmacologic

✉ Dina M. El-Sharawy  
dina.sharawy@nub.edu.eg

✉ Asmaa M. AboulMagd  
asmaa.aboulmaged@nub.edu.eg

<sup>1</sup> Labeled Compounds Department, Hot Lab. Center, Egyptian Atomic Energy Authority (EAEA), P.O. Box 13759, Cairo, Egypt

<sup>2</sup> Radioactive Isotopes and Generators Department, Hot Lab. Center, Egyptian Atomic Energy Authority (EAEA), P. O. Box 13759, Cairo, Egypt

<sup>3</sup> Cyclotron Project, Nuclear Research Center, Cairo, Egypt

<sup>4</sup> Pharmaceutical Chemistry Department, Faculty of Pharmacy, Nahda University, Beni Suef, Egypt

<sup>5</sup> Pharmaceutics and Clinical Pharmacy Department, Faculty of Pharmacy, Nahda University, Beni Suef, Egypt

criteria [14]. It was significant to realize serotonin's influences on normal and abnormal GIT functions. The complete physiological role of serotonin is still unclear, maybe due to different serotonin receptor subtypes in the gut wall and because, according to an *in vivo* study, it has no suitable ligands. Several trials have been conducted for imaging 5-HTRs with  $^{11}\text{C}$  and  $^{18}\text{F}$  [15, 16] using positron emission tomography. Using tracers as SPECT agents is challenging [17, 18]. Among SPECT radioligands, radioactive iodine labeling is one of the favorable techniques because of the superior properties.  $^{125}\text{I}$  is used generally in *in vitro* analyses. In contrast,  $^{131}\text{I}$ ,  $^{124}\text{I}$ , and  $^{123}\text{I}$  can correspondingly be appropriate for radioiodination of serotonin because they have identical chemical properties and provide the same biodistribution profiles. Thus, radioiodination using different iodine radioisotopes covers the imaging potential of these techniques [19]. In this study, serotonin was radiolabeled with  $^{125}\text{I}$  and used as a potential tracer for (5-HTRs) imaging. Different factors are considered in the radiolabeling process that was investigated and optimized to obtain the maximum labeling efficiency. Biodistribution was conducted on animal models of male Swiss albino mice, the activity was determined and calculated as the percentage of injected dose per organ (% ID/organ). Thus, the availability of this tracer for imaging (HTRs) may facilitate the identification and prediction of its mechanism of action and allow the detection and diagnosis of serotonin-related psychiatric diseases and may be a means of measuring selective serotonin reuptake inhibitor occupancy and monitoring of its therapy [20]. In this study, the proposed radiolabeled serotonin was evaluated computationally using the Molecular Operating Environment (MOE) software to comprehend binding interactions between the ligands and receptors in the serotonin receptor binding sites. Additionally, absorption, distribution, metabolism and excretion (ADME) studies were conducted for both serotonin and its radiolabeled analogue.

## 2 Experiment

### 2.1 Material and equipment

#### 2.1.1 Chemicals

In the current study, all chemicals used were of analytical grade. Serotonin and iodogen were acquired from Sigma-Aldrich. Ethanol was used as a solvent. A double distilled water used in all experiments. The chemicals used in buffer preparations were purchased from Riedel-de Haen Seelze-Hannover. The diluted NaOH solution of  $\text{Na}^{125}\text{I}$

(185 MBq/50  $\mu\text{L}$ ) was purchased from Budapest Institute of Isotopes, Hungary.

#### 2.1.2 Equipment

The Nucleus Model 2010  $\gamma$  counter connected with a NaI (TI) crystal was used to measure radioactivity. HPLC (Sykam Model) was performed with a C-18 column (LiChrosorb) (250 mm  $\times$  4–6 mm, 5 mm). The EC-3000 P-series device was used for electrophoresis.

#### 2.1.3 Animals

The study was conducted in compliance with the guidelines established by animal ethics committee of the Egyptian Atomic Energy Authority. Moreover, 30–35-g male Swiss albino mice were purchased from the Agricultural Research Center, Cairo, Egypt. Throughout the experiment, the mice were served with standard suitable nutrition in a stable environment at room temperature ( $22\text{ }^\circ\text{C} \pm 2\text{ }^\circ\text{C}$ ), 12-h light/dark cycle.

## 2.2 Methods

### 2.2.1 Serotonin radiolabeling with $\text{Na}^{125}\text{I}$ using suitable oxidizing agent (iodogen)

Iodogen was placed on the wall of clean brown vials that were dried under the nitrogenous atmosphere as a thin film. Direct iodination reactions were conducted in these cultured tubes. Appropriate serotonin and iodogen amounts were added for radioiodination with 5  $\mu\text{L}$  of  $\text{Na}^{125}\text{I}$  (3.7 MBq); then, the reaction mixture was set aside at different temperatures at different time intervals. The reaction was ended simply by removing the aqueous phase, and to ensure complete termination of the oxidation process,  $\text{Na}_2\text{S}_2\text{O}_5$  was added [21, 22]. Each factor in the radiolabeling process was evaluated with one-way ANOVA, the significance was established at  $P$  value  $> 0.05$ , and the data were presented as mean  $\pm$  standard deviation (SD).

### 2.2.2 Analysis and quality control for radiochemical yield RCY

**2.2.2.1 Thin layer chromatography (TLC) for RCY determination** RCY of  $^{125}\text{I}$ -Ser was determined using previously impregnated aluminum-backed silica gel 60 strips with  $\text{Na}_2\text{S}_2\text{O}_3$  in methylene chloride: ethyl acetate (2:1 v/v) as a developing system. The strips were dried and cut into 1 cm segments and evaluated for radioactivity using  $\gamma$  counter. The free iodide had an  $R_f$  of 0.1, while that of the labeled serotonin was 0.9.

**2.2.2.2 Electrophoresis for RCY analysis** Electrophoresis with EC 3000 power used neutral buffer moistened strips of cellulose acetate, applied the voltage and standing time for 90 min. The strips were dried, cut to 1-cm segments, and counted in  $\gamma$  counter. The RCY was calculated based on the following equation:

$$\%RCY = \frac{\text{Peak activity of } ^{125}\text{I-Ser}}{\text{Total activity}} \times 100$$

**2.2.2.3 HPLC analysis** Using the mobile phase (formic acid, acetonitrile 90:10 v/v, with a flow rate of 1 mL/min and UV at 254 nm [23] in a reversed-phase C<sub>18</sub> column), the eluted fraction of <sup>125</sup>I-Ser at 5 min retention time was collected, dried, and then dissolved in saline solution for injection (Fig. 1).

**2.2.2.4 <sup>125</sup>I-Ser partition coefficient determination** The partition coefficient was determined by centrifuging equal volumes of 1-octanol and <sup>125</sup>I-Ser in phosphate buffer with pH 7.4, in 5000 rpm for 5 min; then, a sample of the aqueous and organic layers were pipetted and counted in a  $\gamma$  counter, it was calculated as log P, which was found to be 1.4 ± 0.2, indicating that <sup>125</sup>I-Ser is a lipophilic tracer, so it can pass through the blood-brain barrier (BBB).

### 2.2.3 Biological distribution studies

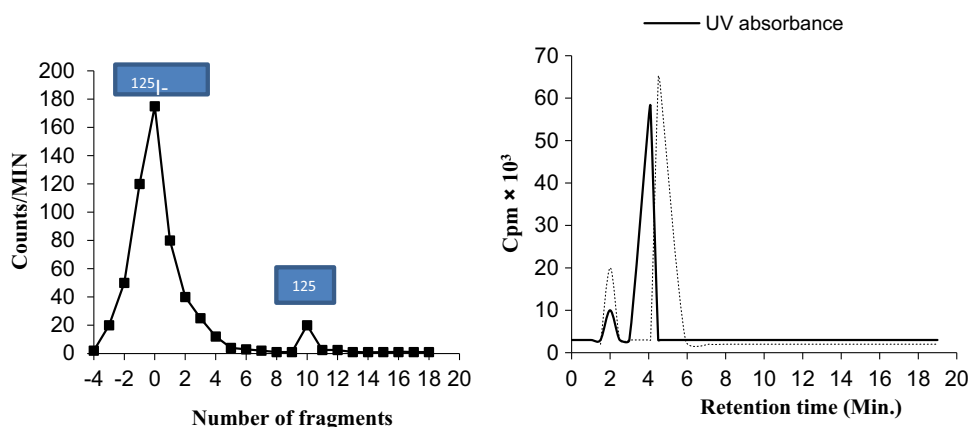
For quantitative biological distribution investigation, male Swiss albino mice were used with an average weight of 30 g each. The mice were housed in a 12-h light/dark cycle, fed by standard distilled water and food pellets. Moreover, 200  $\mu$ L (3.5 MBq) of <sup>125</sup>I-Ser was intravenously injected in the tail vein of the mice. Three mice per group were used for each experiment and housed in suitable conditions of humidity and temperature and supplied with a suitable amount of food and water throughout the experiment. They were sacrificed at 10, 30, 60, and

120 min post-tracer injection. At the sacrifice time, the blood samples were collected, and the remaining organs were isolated, washed, weighed and counted and then compared to a standard solution of labeled serotonin. The average injected dose was calculated per organ. Bone, blood, and muscles were calculated as 10%, 7%, and 40% of the total body weight, respectively [24, 25].

### 2.2.4 Modeling study of the bindings between serotonin and <sup>125</sup>I-Ser to a serotonin receptor

The MOE software was used for docking calculations. The compound's structures were generated by ChemDraw Ultra 11.0. Molecular docking calculations were applied to the serotonin receptor (PDB code 4A6E, <https://www.rcsb.org/pdb/home/home.do>). Docking simulation was performed on the test compounds with the following protocol: (1) The protein structure was checked for missing atoms, bonds, and contacts. (2) Hydrogen atoms were added to the enzyme structure. (3) The ligand molecule was constructed using the builder module and energy minimized. (4) The active site was created using the MOE Alpha Site Finder. (5) The ligand was docked within the serotonin active site using MOEDock with simulated annealing utilized as the search protocol and CHARMM Molecular Mechanics Force Field. (6) The lowest energy conformation of the docked ligand complex was selected and displayed to further energy minimization using the CHARMM force field. To determine the accuracy of this docking protocol, the cocrystallized ligand, was redocked into the serotonin active site. This procedure was repeated three times, and the best ranked solutions of the ligand exhibited root mean standard deviation (RMSD) values of 1.76 Å from the position of the co-crystallized ligand for serotonin. The lowest energy aligned conformations were identified. Thus, this protocol was deemed to be suitable for the docking of both the drug and radiolabeled drug into the active site model of the serotonin complex.

**Fig. 1** Methods of analysis and purification of <sup>125</sup>I-Ser using electrophoresis and HPLC



In silico ADME properties were achieved using PreADMET online program (<https://preadmet.bmdrc.org/>) depending on 2D structural models, drawn in ChemBioDraw Ultra version 11.0 software (Cambridge software).

## 2.3 Results and discussion

### 2.3.1 RCY of $^{125}\text{I}$ -Ser in different pH mediums

The maximum RCY that was achieved (91%) at pH 7 may be attributed to serotonin uptake increase by a factor of 2 between pH 6.8 and pH 7.6 [26]. RCY decreases in the acidic medium (65–74%) due to the predominance of ICI species, which have a lower oxidizing potential effect [27], and in the alkaline medium, RCY was 22–25%. This perhaps ascribed to the reduction in HOI, which is accountable for the substitution reaction [28]. The results are presented in Fig. 2. The highest RCY yield of  $^{125}\text{I}$ -Ser in a neutral medium of pH 7 provides a perfect milieu for direct substitution reaction.

### 2.3.2 RCY of $^{125}\text{I}$ -Ser in different substrate amounts

The maximum RCY (91%) was achieved at 100  $\mu\text{g}$  serotonin (Fig. 2). Lower concentration results in low RCY, and higher concentrations have no significant effect on RCY. This may be attributed to the fact that serotonin reaches the iodonium ion saturation [29] at 100  $\mu\text{g}$ .

### 2.3.3 RCY of $^{125}\text{I}$ -Ser in different IG amounts

To perform an electrophilic substitution reaction, an oxidizing agent as iodogen (1,3,4,6-tetrachloro-3 $\alpha$ ,6 $\alpha$ -diphenylglucoluril) was used, which is responsible for the breakdown of hypochlorite anion to oxidize the iodide  $\text{I}^-$  to iodonium ion  $\text{I}^+$ , which is the active species responsible for substitution reaction on the aromatic ring of serotonin. The significance of different iodogen concentrations on the RCY of  $^{125}\text{I}$ -Ser is shown in Fig. 2. At low IG concentrations, the RCY was low. This may be attributed to insufficient IG to oxidize free iodine, increasing the IG amount to 150  $\mu\text{g}$ . The RCY of  $^{125}\text{I}$ -Ser was increased to 91%. A higher increase in the amount of oxidizing agent decreases the RCY of  $^{125}\text{I}$ -Ser. This may be attributed to the development of undesirable side reactions, such as chlorination [30], polymerization, and denaturation of the substrate.

### 2.3.4 RCY of $^{125}\text{I}$ -Ser in different temperatures

Temperature has a vital effect in electrophilic substitution reactions. The kinetic energy necessary to break down C–H bond and introduce  $\text{I}^+$  into the serotonin phenyl ring was significant when the temperature rises to 60  $^\circ\text{C}$  for 20 min. At room temperature and 40  $^\circ\text{C}$ , it is insufficient to initiate the reaction. The tracer decomposes when the temperature is increased to 100  $^\circ\text{C}$  (Fig. 2). The labeled serotonin was sensitive to high temperature [31, 32], which

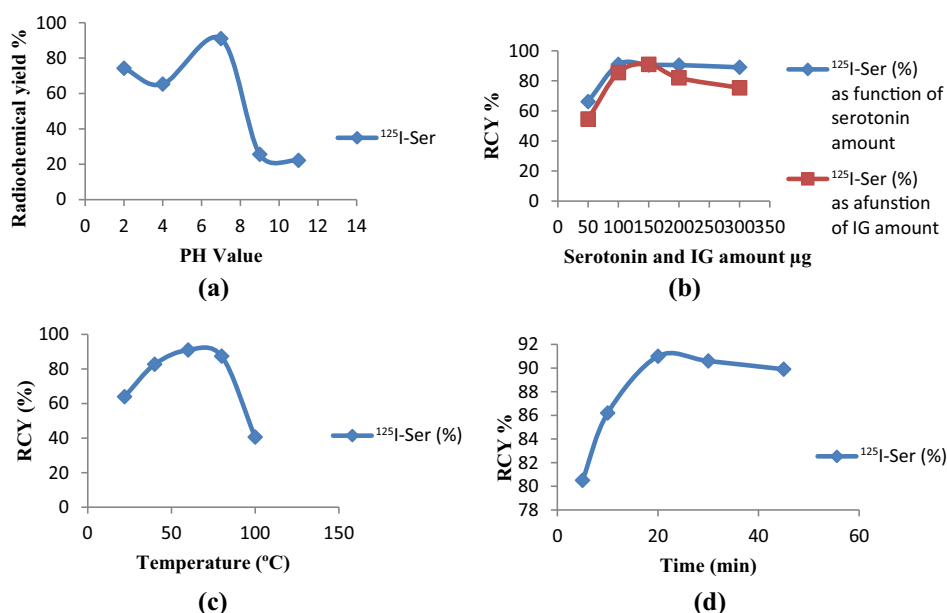


**Fig. 2** Factors affecting radiolabeling of serotonin with radioactive iodine. **a** RCY of  $^{125}\text{I}$ -Ser in different pH mediums 100  $\mu\text{g}$  serotonin, 150  $\mu\text{g}$  iodogen, 100  $\mu\text{L}$  different pH buffers, and 5  $\mu\text{L}$   $\text{Na}^{125}\text{I}$  in 60  $^\circ\text{C}$  for 20 min; **b** RCY of  $^{125}\text{I}$ -Ser in different serotonin and IG amounts X  $\mu\text{g}$  serotonin, X  $\mu\text{g}$  iodogen, 100  $\mu\text{L}$  buffer at pH 7, and 5

$\mu\text{L}$   $\text{Na}^{125}\text{I}$  in 60  $^\circ\text{C}$  for 20 min; **c** RCY of  $^{125}\text{I}$ -Ser in different temperatures, 100  $\mu\text{g}$  serotonin, 150  $\mu\text{g}$  iodogen, 100  $\mu\text{L}$  buffer at pH 7, and 5  $\mu\text{L}$   $\text{Na}^{125}\text{I}$  in ( $X^\circ\text{C}$ ) for 20 min; **d** RCY of  $^{125}\text{I}$ -Ser at different times, 100  $\mu\text{g}$  serotonin, 150  $\mu\text{g}$  iodogen, 100  $\mu\text{L}$  buffer at pH 7, and 5  $\mu\text{L}$   $\text{Na}^{125}\text{I}$  in 60  $^\circ\text{C}$  for X min

might be based on thermal decomposition of the radioligand or degradation of the oxidant.

### 2.3.5 RCY of $^{125}\text{I}$ -Ser at different times

Reaction time has an effective role in building up the energy necessary in C–I bond formation and breaking down C–H bond [33]. As presented in Fig. 2, the minimum time necessary to achieve the highest RCY was 20 min, shorter time was inadequate to introduce all  $^+ \text{I}$  in the phenyl ring, and increasing the time has no valuable effect on the RCY.

### 2.3.6 Tracer in vitro stability

The tracer  $^{125}\text{I}$ -Ser was determined to predict the suitable injection time to prevent any undesirable product results from the radiolysis of the labeled compound, which could be gathered in non-target organs [34]. It was found that the tracer was stable up to 24 h as the RCY was  $91 \pm 3\%$ .

### 2.3.7 Biological distribution

Biological distribution in mice was considered to explain the pathway of the tracer in the body. The samples were collected, washed out, and measured using the  $\gamma$  counter as %ID/organ presented as a mean of the three experiments  $\pm$  SD. Table 1 shows the data after i.v. injection of mice tail vein with 200  $\mu\text{l}$  (3.5 MBq)  $^{125}\text{I}$ -Ser; then, mice were sacrificed after 10, 30, 60, and 120 min postinjection.

The biodistribution clarifies the conjugation of  $^{125}\text{I}$ -Ser with 5HTRs in GIT, and the ratio of the target (GIT) to the

blood was determined. The results were 1.02, 1.78, 2.36, and 4.4, respectively. There is an obvious increase in the ratio indicating that the most suitable time for imaging will be after 2 h of injection as the blood (background) reaches its lowest uptake.

The blood activities were 17%, 10%, 6%, 3%, respectively, postinjection due to the presence of 5HTRs in platelets. Moreover, hepatic stellate cells are present in the liver, and the activities were 12.2%, 10.8%, 6.2%, and 3%, respectively. The uptake of the tracer by the bone decreased rapidly to reach 0.6% after 2 h of injection. The accumulation of the tracer in the heart and lung was low, and washing out was almost complete, as the activity held by the heart after 2 h of the injection was 0.14% and the lung uptake decreased to 0.32%. The tracer was found in a high concentration in the muscle, 19.8% after 10 min of injection, with a slight rapid decline, reaching 6.3% at 2 h postinjection, which may be attributed to the presence of the 5HT<sub>2A</sub> receptor in the skeletal muscle.[35]. The labeled drug is rapidly excreted from the mice through the kidney as almost 70% of the drug was washed out in the urine at 2 h postinjection. The activity of  $^{125}\text{I}$ -Ser in the brain was 0.4% after 10 min postinjection, reaching 0.097% at 2 h postinjection, indicating that the tracer can pass the BBB due to the increase in lipophilicity of the drug by the addition of  $^{125}\text{I}$  [36].

### 2.3.8 Docking study

It is obvious that the binding energy of serotonin (–9.945 kcal/mol) is less than that of radiolabeled analog (–11.001 kcal/mol) and indicates higher affinity of the radiolabeled drug to the receptor (Table 2). The best docking poses for both ligands are presented in Fig. 3. It shows that

**Table 1.**  $^{125}\text{I}$ -Ser biological distribution in normal mice

| Organ     | Time            |                 |                   |                    |
|-----------|-----------------|-----------------|-------------------|--------------------|
|           | 10 min          | 30 min          | 1 h               | 2 h                |
| Blood     | 17.4% $\pm$ 1.1 | 10% $\pm$ 0.9   | 6% $\pm$ 0.8      | 3% $\pm$ 0.1       |
| Muscle    | 19.8% $\pm$ 1.3 | 14% $\pm$ 1.1   | 10% $\pm$ 0.6     | 6.3% $\pm$ 0.2     |
| Bone      | 8.6% $\pm$ 0.8  | 4.4% $\pm$ 0.2  | 2.7% $\pm$ 0.2    | 0.6% $\pm$ 0.01    |
| Spleen    | 3% $\pm$ 0.1    | 1.1% $\pm$ 0.01 | 0.6% $\pm$ 0.01   | 0.3% $\pm$ 0.01    |
| Liver     | 12.2% $\pm$ 0.2 | 10.8% $\pm$ 0.8 | 6.2% $\pm$ 0.1    | 3% $\pm$ 0.1       |
| Stomach   | 2.1% $\pm$ 0.01 | 3.1% $\pm$ 0.03 | 4.2% $\pm$ 0.1    | 6.6% $\pm$ 0.2     |
| Intestine | 15.7% $\pm$ 0.4 | 14.7% $\pm$ 0.9 | 10% $\pm$ 0.9     | 6.7% $\pm$ 0.3     |
| Kidney    | 8% $\pm$ 0.5    | 4.1% $\pm$ 0.1  | 3.3% $\pm$ 0.01   | 1.2% $\pm$ 0.01    |
| Lung      | 1.7% $\pm$ 0.03 | 2.1% $\pm$ 0.02 | 0.6% $\pm$ 0.02   | 0.32% $\pm$ 0.01   |
| Heart     | 1.5% $\pm$ 0.02 | 0.9% $\pm$ 0.01 | 0.3% $\pm$ 0.01   | 0.14% $\pm$ 0      |
| Urine     | 9% $\pm$ 0.7    | 35.5% $\pm$ 1.5 | 56% $\pm$ 1.3     | 71.7% $\pm$ 1.4    |
| Brain     | 0.4% $\pm$ 0.05 | 0.1% $\pm$ 0.02 | 0.07% $\pm$ 0.003 | 0.097% $\pm$ 0.001 |
| GIT/blood | 1.02 $\pm$ 0.01 | 1.78 $\pm$ 0.01 | 2.36 $\pm$ 0.02   | 4.43 $\pm$ 0.02    |

**Table 2** Ranking results of serotonin binding energy and  $^{125}\text{I}$ -Ser–serotonin complex binding conformations

| Compound name         | Binding energy score | The average number of poses per run |
|-----------------------|----------------------|-------------------------------------|
| Serotonin             | −9.945               | 10                                  |
| $^{125}\text{I}$ -Ser | −11.001              | 9                                   |

\* The score is the mean of three consecutive runs

\* The docking method was validated by a successful pose-retrieval docking experiment of the ligand (score: −9.618)

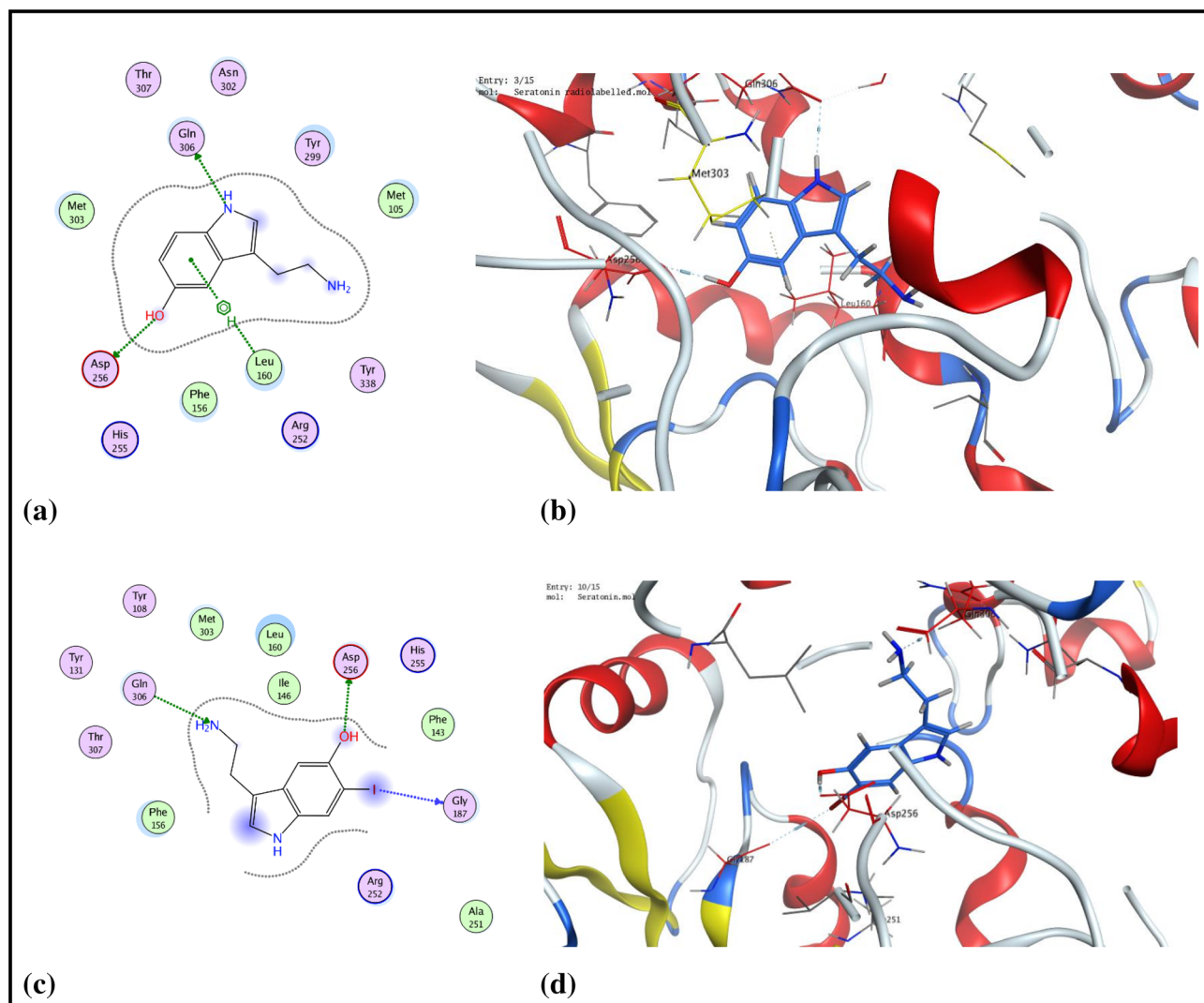


**Fig. 3** (Color online) **a** Computer modeling of serotonin binding to serotonin receptor (4A6E). **b** 3D caption of serotonin binding to its receptor. Serotonin was colored in blue. **c** The 2D caption of  $^{125}\text{I}$ -Ser

binding to the active site of serotonin. **d** The binding pattern of  $^{125}\text{I}$ -Ser colored by the element, ball, and stick into the receptor-binding site showing three interactions (dotted lines)

serotonin binds with two hydrogen bond interactions with amino acid residues Gln 306 and Asp 256 and with hydrophobic interaction with Leu 160 amino acid. Furthermore,  $^{125}\text{I}$ -Ser showed the same binding interaction of the ligand with Gln 306 amino acid and Asp 256 in addition to an additional binding interaction with Gly 187, which binds to the iodine of serotonin.

### 2.3.9 *In silico* molecular and ADME properties

ADME/Tox issues are the greatest challenging part in many drug discovery projects as pharmacokinetic (ADME) and pharmacodynamic (e.g., toxicological) properties (drug-likeness) are of valuable importance during preclinical evaluation to optimize a lead compound into a

successful drug candidate and decrease the exhaustion rates in clinical trials. It is important in the pharmaceutical sphere to study the BBB as some active drugs pass through it. Proper neuronal function is controlled by the BBB, which is an essential barrier. This barrier is considered an important key to determine treatments for various neurological diseases. The pathophysiology of many diseases is caused by the disruption of the BBB and because crossing the BBB is a fundamental consideration in CNS-acting therapeutics. Recent studies have designed many molecules required for BBB function in addition to some molecular signaling events that control the formation of the BBB during progression and its reaction to injury and disease. Moreover, one of the key physicochemical parameters for identifying possible drug candidate is human intestinal absorption (HIA%) [37]. Oral bioavailability has a significant consideration regarding the progress of bioactive therapeutic agents. Therefore, an effective in vitro Caco-2 cell model and Madin-Darby canine kidney (MDCK) cell model are suggested to estimate the oral bioavailability [38]. The health hazard that emerges from toxic skin exposure to chemicals was evaluated by determining the permeation coefficient (Kp) used for prediction of the dermal penetration of chemicals [39].

The values shown in Table 3 indicate that BBB of the three proposed <sup>125</sup>I-Ser structures showed relatively higher BBB (1.821–1.822) compared to serotonin (1.149), and this contributes to the hydrophobic nature of the iodine atom of the <sup>125</sup>I-Ser. Additionally, the binding affinity of serotonin, which is indicated by 8.631, is much lower than that of the radiolabeled analog. Regarding the HIA%, serotonin reveals lower HIA (84.120) than the radiolabeled derivative (93.381). Furthermore, serotonin showed lower Caco-2 and higher MDCK than the radiolabeled derivatives. Finally, SP (logKp) of <sup>125</sup>I-Ser showed relatively higher values (range, -4.007 to 4.127) compared to unlabeled serotonin (-4.258).

**Table 3** ADME properties of the studied compounds obtained using the in silico method

| Molecule            | Serotonin | Cpd1   | Cpd 2  | Cpd 3  |
|---------------------|-----------|--------|--------|--------|
| BBB (Cbrain/Cblood) | 1.149     | 1.822  | 1.821  | 1.822  |
| PPB                 | 8.631     | 15.127 | 67.400 | 34.871 |
| HIA%                | 84.120    | 93.381 | 93.381 | 93.381 |
| Caco-2 (nm/s)       | 12.178    | 17.478 | 17.792 | 17.793 |
| MDCK (nm/s)         | 38.650    | 0.500  | 0.495  | 0.497  |
| SP (logKp)          | -4.258    | -4.125 | -4.127 | -4.007 |

### 3 Conclusion

Based on the previous study, radiolabeling of serotonin was conducted by electrophilic substitution reaction using 100 µg serotonin, 150 µg Ig as oxidizing agent, 100 µL buffer at pH 7, and 5 µL Na<sup>125</sup>I in 60°C for 20 min. All parameters of the reaction were used to optimize RCY up to 91%. The radioactive tracer <sup>125</sup>I-Ser had in vivo and in vitro stability. Moreover, computational evaluation of serotonin and its radiolabeled analog was performed using the MOE software, which includes molecular docking and ADME studies. The biodistribution shows the possibility of using <sup>125</sup>I-Ser tracer for imaging serotonin receptors in the GIT and brain due to its high binding affinity to 5HTRs, which provides an auspicious vision in the determination of receptor's function and relationship to the disease.

### References

- Z. Li, A. Chalazonitis, Y.Y. Huang et al., Essential roles of enteric neuronal serotonin in gastrointestinal motility and the development/survival of enteric dopaminergic neurons. *J. Neurosci.* **31**, 8998–9009 (2011). <https://doi.org/10.1523/JNEUROSCI.6684-10>
- N. Terry, K.G. Margolis, serotonergic mechanisms regulating the GI tract: experimental evidence and therapeutic relevance. *Handb. Exp. Pharmacol.* **239**, 319–342 (2017). [https://doi.org/10.1007/164\\_2016\\_103](https://doi.org/10.1007/164_2016_103)
- K.O. Grönstad, L. DeMagistris, A. Dahlström et al., The effects of vagal nerve stimulation on endoluminal release of serotonin and substance P into the feline small intestine. *J. Scand. Gastroenterol.* **20**, 163–169 (1985). <https://doi.org/10.3109/00365528509089650>
- J.J. Chen, L.I. Zhishan, H. Pan et al., Maintenance of serotonin in the intestinal mucosa and ganglia of mice that lack the high-affinity serotonin transporter: abnormal intestinal motility and the expression of cation transporters. *J. Neurosci.* **21**, 6348–6361 (2001). <https://doi.org/10.1523/JNEUROSCI.21-16-06348>
- E. Büllbring, A. Creema, The release of 5-hydroxytryptamine in relation to pressure exerted on the intestinal mucosa. *J. Physiol.* **146**, 18–28 (1959). <https://doi.org/10.1113/jphysiol.1959.sp006175>
- P.P. Bertrand, Real-time detection of serotonin release from enterochromaffin cells of the guinea-pig ileum. *Neurogastroenterol. Motil.* **16**, 511–514 (2004). <https://doi.org/10.1111/j.1365-2982.2004.00572.x>
- H. Schwörer, K. Racké, H. Kilbinger, Cholinergic modulation of the release of 5-hydroxytryptamine from the guinea pig ileum. *Naunyn-Schmiedeberg's Arch. Pharmacol.* **336**, 127–132 (1987). <https://doi.org/10.1007/BF00165795>
- K. Racké, A. Reimann, H. Schwörer et al., Regulation of 5-HT release from enterochromaffin cells. *Behav. Brain. Res.* **73**, 83–87 (1996). [https://doi.org/10.1016/0166-4328\(96\)00075-7](https://doi.org/10.1016/0166-4328(96)00075-7)
- M.D. Gershon, Nerves reflexes and the enteric nervous system: pathogenesis of the irritable bowel syndrome. *J. Clin. Gastroenterol.* **39**, 184–193 (2005). <https://doi.org/10.1097/01.mcg.0000156403.37240.30>

10. V. Erspamer, *Occurrence of indolealkylamines in nature. Handbook of experimental pharmacology*, vol. 19 (Springer, New York, 1966), pp. 132–181
11. M.D. Gershon, The serotonin signaling system: from basic understanding to drug development for functional GI disorders. *J. Gastroenterol.* **132**, 397–414 (2007). <https://doi.org/10.1053/j.gastro.2006.11.002>
12. M.D. Gershon, 5-Hydroxytryptamine (serotonin) in the gastrointestinal tract. *Curr. Opin. Endocrinol. Diabetes Obes.* **20**, 14–21 (2013). <https://doi.org/10.1097/MED.0b013e32835bc703>
13. M. Vialli, *Histology of the enterochromaffin cell system. Handbook of experimental pharmacology*, vol. 19 (Springer, New York, 1966), pp. 1–65
14. L. Lemoine, J. Andries, D.L. Bars et al., Comparison of 4 radiolabeled antagonists for serotonin 5-HT<sub>7</sub> receptor neuroimaging: toward the first PET radiotracer. *J. Nucl. Med.* **52**, 1811–1818 (2011). <https://doi.org/10.2967/jnumed.111.089185>
15. B. Vidal, S. Fieux, M. Colom et al., 18F–F13640 preclinical evaluation in rodent, cat and primate as a 5-HT<sub>1A</sub> receptor agonist for PET neuroimaging. *Brain Struct. Funct.* **223**, 2973–2988 (2018). <https://doi.org/10.1007/s00429-018-1672-7>
16. L.M. Paterson, B.R. Kornum, D.J. Nutt et al., 5-HT radioligands for human brain imaging with PET and SPECT. *Med Res Rev.* **33**, 54–111 (2013). <https://doi.org/10.1002/med.20245>
17. G.B. Meerveld, K. Venkova, G. Hicks et al., Activation of peripheral 5-HT receptors attenuates colonic sensitivity to intraluminal distension. *Neurogastroenterol. Motil.* **18**, 76–86 (2006). <https://doi.org/10.1111/j.1365-2982.2005.00723.x>
18. L.M. Paterson, R.J. Tayak, D.J. Nutt et al., Measuring endogenous 5-HT release by emission tomography: promises and pitfalls. *J. Cereb. Blood Flow Metab.* **30**, 1682–1706 (2010). <https://doi.org/10.1038/jcbfm.2010.104>
19. S.N. Farrag, A. Hanan, E.M. Abdulaziz et al., Comparative study on radiolabeling and biodistribution of core-shell silver/polymeric nanoparticles-based theranostics for tumor targeting. *Int. J. Pharm.* **529**, 123–133 (2017). <https://doi.org/10.1016/j.ijpharm.2017.06.044>
20. F. Côté, E. Thévenot, C. Fligny et al., Disruption of the non-neuronal tph1 gene demonstrates the importance of peripheral serotonin in cardiac function. *Proc. Natl. Acad. Sci. USA* **100**, 13525–13530 (2003). <https://doi.org/10.1073/pnas.2233056100>
21. S.N. Farrag, A.O. Abdel Moamen, Facile radiolabeling optimization process via design of experiments and an intelligent optimization algorithm: application for omeprazole radioiodination. *J. Label Compd. Radiopharm.* **62**, 280–287 (2019). <https://doi.org/10.1002/jlcr.3734>
22. M.A. Motaleb, M.T. El-Kolaly, H.M. Rashed et al., Radioiodinated paroxetine, a novel potential radiopharmaceutical for lung perfusion scan. *J. Radioanal. Nucl. Chem.* **292**, 629–635 (2012). <https://doi.org/10.1007/s10967-011-1499-7>
23. J. Thomas, R. Khanam, D. Vohora, A validated HPLC-UV method and optimization of sample preparation technique for norepinephrine and serotonin in mouse brain. *J. Pharmaceutical. Biol.* **53**, 1539–1544 (2015). <https://doi.org/10.3109/13880209.2014.991837>
24. M.H. Sanad, M. El-Tawoosy, Labeling of ursodeoxycholic acid with technetium-99m for hepatobiliary imaging. *J. Radioanal. Nucl. Chem.* **298**, 1105–1109 (2013). <https://doi.org/10.1007/s10967-013-2512-0>
25. B.S. Challan, A. Massoud, Radiolabeling of graphene oxide by Technetium-99m for infection imaging in rats. *J. Radioanal. Nucl. Chem.* **314**, 2189–2199 (2017). <https://doi.org/10.1007/s10967-017-5561-y>
26. T. Sharma, L.S. Guski, N. Freund et al., Suicidality and aggression during antidepressant treatment: systematic review and meta-analyses based on clinical study reports. *BMJ* **352**, i65 (2016). <https://doi.org/10.1136/bmj.i65>
27. A.M. Amin, N.S. Farrag, A. AbdEl-Bary, Iodine-125-chlorambucil as possible radio anticancer for diagnosis and therapy of cancer: preparation and tissue distribution. *B J P R* **4**, 1873–1885 (2014). <https://doi.org/10.9734/BJPR/2014/10520>
28. A.M. Amin, A. Abd El-Bary, M. Shoukry, Shoukry Study of the conditions for ibuprofen labeling with <sup>125</sup>I to prepare an inflammation imaging agent. *J. Radiochem.* **55**, 615–619 (2013). <https://doi.org/10.1134/S106636221306009X>
29. K.M. El-Azony, A.A. El-Mohty, H.M. Killa et al., An investigation of the <sup>125</sup>I-radioiodination of colchicine for medical purposes. *J. Labelled. Compds. Radiopharm.* **52**, 1–3 (2008). <https://doi.org/10.1002/jlcr.1556>
30. K. El-Azony, Preparation of <sup>125</sup>I-celecoxib with high purity as a possible tumor agent. *J. Radioanal. Nucl. Chem.* **285**, 315–320 (2010). <https://doi.org/10.1007/s10967-010-0583-8>
31. A. Braganza, W.O. Wilson, Elevated temperature effects on catecholamines and serotonin in brains of male Japanese quail. *J Appl. Physiol. Respir. Environ. Exerc. Phys.* **45**, 705–708 (1978). <https://doi.org/10.1152/jappl.1978.45.5.705>
32. B.M. Essa, T.M. Sakr, M.A. Khedr et al., <sup>99m</sup>Tc-amitrol as a novel selective imaging probe for solid tumor: in Silico and preclinical pharmacological study. *J Eur Pharm Sci.* **76**, 102–109 (2015). <https://doi.org/10.1016/j.ejps.2015.05.002>
33. E.J. Knust, K. Dutschk, Radiopharmaceutical preparation of 3–123I- $\alpha$ -methyltyrosine for nuclearmedical applications. *J. Radioanal. Nucl. Chem.* **144**, 107–113 (1990)
34. H.M. Rashed, I.T. Ibrahim, M.A. Motaleb, A. Abd El-Bary, Preparation of radioiodinated ritodrine as a potential agent for lung imaging. *J. Radioanal. Nucl. Chem.* **300**, 1227–1233 (2014). <https://doi.org/10.1007/s10967-014-3077-2>
35. S. G-Deniau, A.F. Burnol, J. Girard, Identification and localization of a skeletal muscle serotonin 5-HT<sub>2A</sub> receptor coupled to the Jak/STAT Pathway. *J. Biol. Chem.* **272**, 14825–14829 (1997). <https://doi.org/10.1074/jbc.272.23.14825>
36. N.R. Waterhouse, Determination of lipophilicity and its use as a predictor of blood-brain barrier penetration of molecular imaging agents. *Mol. Imag. Biol.* **5**, 376–389 (2003). <https://doi.org/10.1016/j.mibio.2003.09.014>
37. Y.H. Zhao, M.H. Abraham, Evaluation of human intestinal absorption data and subsequent derivation of a quantitative structure-activity relationship (QSAR) with the Abraham descriptors. *J. Pharm. Sci.* **90**, 749–784 (2001). <https://doi.org/10.1002/jps.1031>
38. T.J. Hou, W. Zhang, ADME evaluation in drug discovery. Correlation of caco-2 permeation with simple molecular properties. *J. Chem. Inf. Comput. Sci.* **44**, 1585–1600 (2004). <https://doi.org/10.1021/ci049884m>
39. Y.C. Chang, C.P. Chen, C.C. Chen, 2012 International symposium on safety science and technology predicting skin permeability of chemical substances using a quantitative structure-activity relationship. *Proc. Eng.* **45**, 875–879 (2012). <https://doi.org/10.1016/j.proeng.2012.08.252>